Crystal-field-induced spin rotations in $NdCo_2$ and $HoCo_2$: A Mössbauer study

U. Atzmony,* M. P. Dariel,*† and G. Dublon
Nuclear Research Centre–Negev, Post Office Box 9001, Beer-Sheva, Israel
(Received 23 February 1976)

The magnetic anisotropy properties of ^{57}Fe-doped $NdCo_2$ and $HoCo_2$ were studied by means of Mössbauer spectroscopy in the 4.2–300 K temperature range. The experimental results indicate the presence of spin reorientations taking place at 43.5 and 16 K, for $NdCo_2$ and $HoCo_2$, respectively. Single-ion-model crystal-field calculations account for the experimental results and allow the determination of the crystal-field parameters.

I. INTRODUCTION

The cubic Laves-phase compounds RM_2, where R is a rare-earth metal and M = Al, Fe, Co, or Ni, display a variety of interesting properties of magnetic origin.[1] These properties depend on the exchange interactions and the crystalline-electric-field (CEF) effects, both of which can be varied substantially by changing the R and M components.

The objective of the present study was to investigate by means of Mössbauer spectroscopy the nature of previously reported transitions in[2] $NdCo_2$ and[3] $HoCo_2$. Apart from the magnetic order-disorder transitions at T_C,[4,5] specific-heat measurements revealed the presence of additional thermal anomalies occurring at 42 and 16 K in $NdCo_2$ and $HoCo_2$, respectively.

The two Laves compounds $NdCo_2$ and $HoCo_2$ differ in the relative strength of the exchange and CEF effects.[2-10] In $NdCo_2$ CEF effects produce a quenched Nd^{3+} moment of about $1.8\mu_B$.[6,7] The Ho^{3+} moment in $HoCo_2$ is close to its free-ion value of $10\mu_B$.[6,8-10] The two compounds also differ in the relative alignment of the sublattice magnetizations. For Nd, a light rare earth, $J = L - S$, while for the heavy rare earth Ho, $J = L + S$. The spin angular momenta of the R ions are coupled antiparallel to those of the M ions.[1] This leads to ferromagnetic ordering of the moments in $NdCo_2$,[9] and to ferrimagnetism in $HoCo_2$.[2] Neutron-diffraction measurements[9] did not reveal any change in either the crystalline or the magnetic structure of the two compounds below their respective T_C. The specific-heat anomalies[2,3] can be reconciled with the neutron-diffraction results,[9] if they are assigned to spin-reorientation-like transitions. A change of the axis of easy magnetization is not detectable by powder neutron diffraction of a cubic material.[11]

Temperature-dependent axes of easy magnetization $\vec{n}$ have been observed previously in binary $SmFe_2$,[12] $CeFe_2$,[13] and $HoFe_2$,[14] and in some ternary cubic Laves $R^1_{1-x}R^2_x\,Fe_2$ compounds.[11,15] In $SmFe_2$, $\vec{n}$ rotates continuously within the $(1\bar{1}0)$ plane, from the [110] to the [111] axis. The spin-rotation temperature interval is ~100 K wide and is well below T_C. The directions which $\vec{n}$ assumes in this interval, namely, not parallel to a major axis of cubic symmetry but contained in the $(1\bar{1}0)$ plane, are $[uuw]$ directions. The spin rotation in $CeFe_2$ is also of the $[uuw]$ type and extends over a similarly wide temperature range. It, however, terminates at T_C, 30° away from the [110] axis. In $HoFe_2$,[14] $\vec{n}$ is observed to rotate away from the [100] towards the [110] axis, below 14 K. Similar phenomena, though of various temperature dependences, have been detected in the ternary $R^1_{1-x}R^2_x\,Fe_2$ compounds.[11,15] The reorientation of the axis of easy mangetization $\vec{n}$, from one major axis of cubic symmetry to another was described in terms of the single rare-earth ion model.[12-16] The experimentally determined spin-orientation diagrams of the pseudobinary $R^1_{1-x}R^2_x\,Fe_2$ systems with heavy-rare-earth elements were successfully accounted for, using constant crystal-field parameters A_4 and A_6 and a small fixed contribution to the anisotropy energy attributed to the Fe-Fe interaction. The single-ion model was also used to describe the spin reorientation in $SmFe_2$,[16] in this case, however, significantly larger values of A_4 and A_6 had to be employed.

The occurrence of $[uuw]$- and $[uv0]$-type axes of magnetization could be accounted for within the framework of the phenomenological treatment of the magnetic anisotropy free energy.[13] This treatment required the inclusion of a third-order anisotropy constant in the expression for the free energy. Recent calculations[17] showed that the non-major cubic symmetry axes of easy magnetization can be derived in the framework of the single-ion model, for certain combinations of the crystal-field parameters and the exchange fields. In particular, these calculations successfully reproduced the observed spin rotation in $HoFe_2$ at low temperature.[14,17]

The Mössbauer effect of ^{57}Fe is a highly effective tool in the study of magnetic-anisotropy ef-

fects in cubic Laves compounds.[12-16] Data on the spin reorientations can in turn be used to gain insight into crystal-field effects and to determine crystal-field parameters. The present work represents the first effort to apply this technique to the study of $R\mathrm{Co}_2$ compounds.

II. EXPERIMENTAL TECHNIQUES

The compounds $\mathrm{Nd}(\mathrm{Co}_{1-\epsilon}{}^{57}\mathrm{Fe}_\epsilon)_2$ and $\mathrm{Ho}(\mathrm{Co}_{1-\epsilon}{}^{57}\mathrm{Fe}_\epsilon)_2$, with $\epsilon < 0.05$, were prepared by arc melting on a water-cooled copper hearth, stoichiometric amounts of 99.9% pure rare earth, 99.99% pure Co and 80-at.% isotopically enriched ^{57}Fe. Several compounds, with $0.01 < \epsilon < 0.05$, were prepared in order to check for possible variations of the magnetic or structural properties of the $R\mathrm{Co}_2$ compounds due to the presence of small amounts of iron. The arc-cast samples were annealed in evacuated (10^{-5}-Torr) quartz capsules at 600 °C for 14 days. The homogenized samples were subsequently analyzed by means of powder x-ray diffraction (Cr $K\alpha$) and by electron microprobe analysis. Less than 1% of foreign phases were observed and the compositional homogeneity was within 0.5%. The lattice parameters of the ^{57}Fe containing NdCo_2 and HoCo_2 were in good agreement with previously reported values of the iron-free compounds. Variations of the lattice parameter as a function of the iron concentration in the (2–10)-at.% range were less than 0.05%.

The Mössbauer-effect measurements were carried out using a constant-acceleration-type spectrometer with a 15-mC ^{57}Co-Pt source. The 14.4-keV γ-ray transition of ^{57}Fe was detected after passing through 300-mesh 22-mg/cm^2 $\mathrm{NdCo}_2(^{57}\mathrm{Fe})$ or $\mathrm{HoCo}_2(^{57}\mathrm{Fe})$ absorbers. The temperature was stabilized to within 0.5 K in helium or nitrogen flow cryostats, within the 4.2–300-K temperature range.

The presence of the low-^{57}Fe concentration increases slightly the Curie temperatures of NdCo_2 and HoCo_2. The Mössbauer-effect measurements in the present study showed Curie points of 125 ± 2 and 95 ± 2 K for the iron-containing NdCo_2 and HoCo_2, respectively, as compared with[2,4] $T_C = 116$ or[6] 98 K for NdCo_2 and $T_C = 87$ or[3] 77 K for HoCo_2. In the course of the present study, the transitions in the magnetically ordered state were observed to occur at 43.5 ± 0.5 and 16 ± 1 K as compared with the reported values of[2] 42 and[3,5] 16 K for NdCo_2 and HoCo_2, respectively. These transition temperatures were observed to be independent of the iron content in the (2–10)-at.% Fe range. Moreover, ultrasonic measurements[18] of iron-free $R\mathrm{Co}_2$ compounds, which had been prepared as described above, revealed elastic anomalies at 120 and 43 K for NdCo_2, and at 90 and 16 K for HoCo_2. Neutron-diffraction measurements of polycrystalline NdCo_2 did not reveal any structural or magnetic phase changes below T_C,[19] in agreement with previous studies.[9] These findings indicate that the ^{57}Fe additions randomly occupy Co sites and exert little effect only on the magnetic properties.

III. MÖSSBAUER-SPECTRA FITTING PROCEDURES

The interpretation of the Mössbauer spectra follows the pattern employed in previous studies of spin rotations in SmFe_2,[12] CeFe_2,[13] and $\mathrm{Ho}_x\mathrm{Er}_{1-x}\mathrm{Fe}_2$.[15] The direction of the magnetization $\vec{n}$ relative to the cubic cell axes of the $R\mathrm{Co}_2$-^{57}Fe compounds, determines the number of the inequivalent iron (i.e., cobalt) sites and their population ratio, as listed in Table I. A detailed description of the least-squares computer fitting procedure for one-, two-, or three-site ^{57}Fe Mössbauer spectra was given elsewhere.[13] It takes into account the angle between the direction of the magnetic exchange field and the CEF gradient. The computer program calculates the positions and intensities of the absorption lines by diagonalizing the Hamiltonian for each inequivalent site. It is assumed that (i) the effective magnetic field is parallel to $\vec{n}$, (ii) all inequivalent iron sites possess the same isomer shift and quadrupole constant $\frac{1}{4}eqQ$, but differ in the value of the magnetic hyperfine constant $g_0\mu_n\vec{H}_{\mathrm{eff}}$; (iii) the quadrupole constant is the sum of a lattice field contribution, with an axis of symmetry parallel to the local axis of symmetry and a magnetically induced contribution with an axis parallel to the effective field $\vec{H}_{\mathrm{eff}}$; and (iv) the absorption lines have a Lorentzian shape and equal width at half-maximum Γ_0. The fitting procedure described above will be referred to as procedure I.

Fitting procedure I did not yield satisfactory simulations of the NdCo_2-^{57}Fe Mössbauer spectra below 43.5 K (Fig. 1). For these spectra a simpler fitting procedure was used. It will be re-

TABLE I. Easy axes of magnetization in cubic Laves phase $R\mathrm{Co}_2$-^{57}Fe and corresponding number of inequivalent iron sites and population ratio.

Easy axis of magnetization	Number of inequivalent iron sites	Population ratio
[100]	1	
[110]	2	2 : 2
[111]	2	3 : 1
[uuw]	3	2 : 1 : 1
[uvw]	4	1 : 1 : 1 : 1

ferred to as procedure II. It assumes that the spectra were superpositions of two six-line ^{57}Fe patterns. The main fitting parameters were (a) the electric quadrupole and the effective hyperfine field constants of each Hamiltonian; (b) the linewidth at half-maximum of a single absorption line Γ_0, common to all lines; and (c) the isomer shift and relative intensity R of one of the superimposed patterns (that of the second pattern being $1-R$). The effectiveness of least-squares-fitting procedure II was checked by applying it to [111]-, [110]-, and [100]-type ^{57}Fe-spectra. Identical values of the hyperfine effective fields, the isomer shift, the linewidth, and the relative intensities of inequivalent iron sites were obtained by both procedures, I and II. The only difference between the two fitting procedures was the value obtained for the electric quadrupole constant, $\frac{1}{4}eqQ$. Procedure II yields different values of this constant for each inequivalent site. This should be expected from first-order calculations, an example of which will be given below. For a [111]-type Mössbauer spectrum, procedure II yields $(\frac{1}{4}eqQ)_1$ for the low-intensity site, which is in agreement with the quadrupole constant obtained following procedure I. The value for the high-intensity site is approximately $\frac{1}{3}(\frac{1}{4}eqQ)_1$. Assuming an angle between the hyperfine effective field and the electric field gradient, the first-order approximation to the quadrupole interaction is $\frac{1}{4}eqQ[(3\cos^2\theta-1)/2]$. For a [111] spectrum, the axis of local symmetry of three (out of four) iron sites, forms an angle $\theta=\cos^{-1}\frac{1}{3}$ with the direction of H_{eff}. The lattice quadrupole contribution in this case is thus equal to $-\frac{1}{3}(\frac{1}{4}eqQ)$. The axis of local symmetry of the fourth site is parallel to $\vec{H}_{eff}$, for the [111] direction of $\vec{n}$, and thus $\frac{1}{4}eqQ[(3\cos^2\theta-1)/2]=\frac{1}{4}eqQ$. Similar results are obtained by procedure II fits when applied to [110] spectra. Though procedure I is more sophisticated and physically sounder, procedure II yields satisfactory results as long as $\mu_n g_0 H_{eff} > \frac{1}{4}eqQ$.

IV. RESULTS AND ANALYSIS

A. $NdCo_2$

A cursory study of the Mössbauer spectra of ^{57}Fe in $NdCo_2$ reveals the presence of three temperature-dependent magnetic states and corresponding transition regions. Below 43.5 K complex spectra were recorded which imply the presence of more than one iron site. Since the iron atoms occupy the Co sites, and excluding the possibility of a noncubic structure below 43.5 K,[9,19] these spectra indicate an axis of easy magnetization other than [100].[13] A typical spectrum of this kind at 20 K is shown in Fig. 1. In Fig. 2, spectra taken between 43.5 and 45 K are shown, displaying a sharp ordered-state magnetic transition in $NdCo_2$. The 45-K six-line pattern, as well as the other obtained spectra for $45 \leq T \leq 110$ K, are characteristic of a single iron site and interpretable in terms of a [100] easy axis of magnetization. Mössbauer spectra showing the magnetic order-disorder transition are presented in Fig. 3. This transition extends over a ~15-K interval in which the magnetic hyperfine effective fields decrease rapidly and the one-iron site appearance becomes blurred or is completely lost. The absorption doublet at 125 K is characteristic of an iron ion in an electric field gradient. In the 120-K spectrum (Fig. 3), which is essentially a doublet, the small wings are noteworthy. These wings possibly reflect a weak, fluctuating spin polarization caused by the ^{57}Fe moments. The slight increase of T_C, as compared with that of iron-free $NdCo_2$,[2,4] can be attributed to the presence of the iron impurities. Changes in the Mössbauer properties of $NdCo_2$-^{57}Fe, as a function of the ^{57}Fe content in the (2–10)-at.% range, were found to be negligible.

Three computer simulations of the 20-K Mössbauer spectrum of $NdCo_2$-^{57}Fe are shown in Fig. 1.

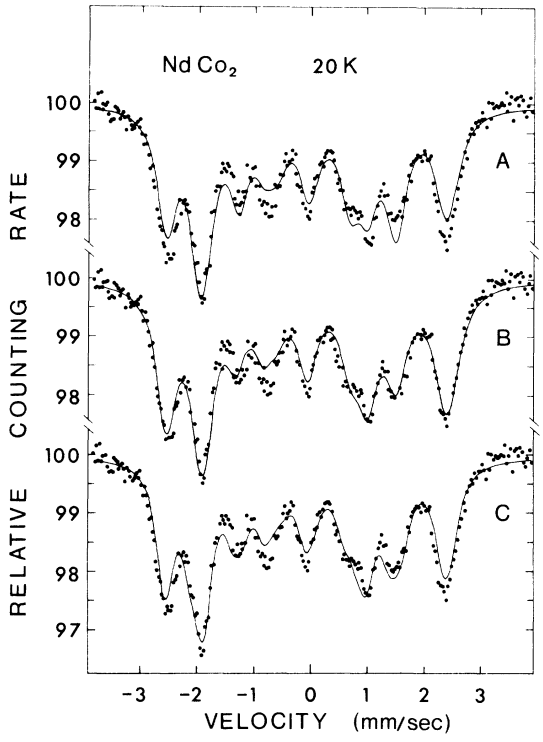

FIG. 1. Mössbauer spectrum of $NdCo_2$-^{57}Fe at 20 K. The full lines through the experimental points are least-squares computer fits: (A) [110] procedure I type; (B) two-sites procedure II type; and (C) [*uuw*] procedure I type.

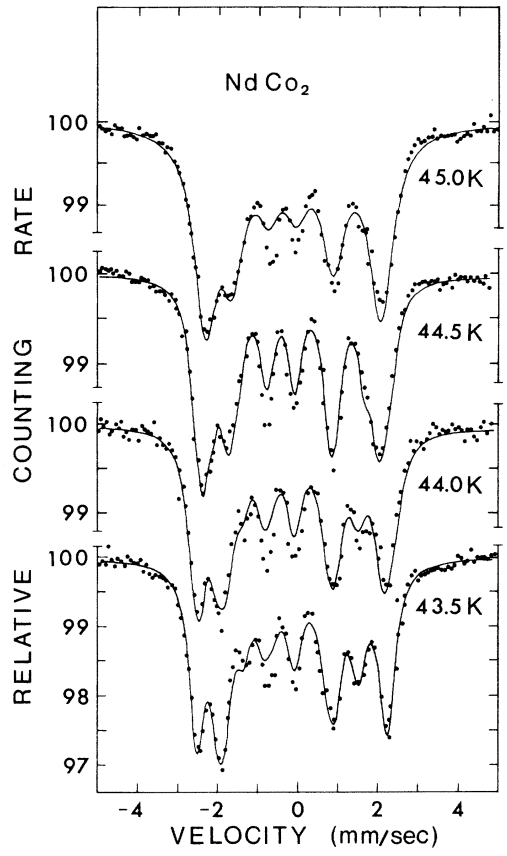

FIG. 2. Mössbauer spectra of $NdCo_2$-^{57}Fe between 43.5 and 45 K. The presented least-squares fits (full lines) are two-site procedure II type at 43.5 K; [*uuw*] procedure I type at 44 and 44.5 K; and [100] procedure I type at 45 K.

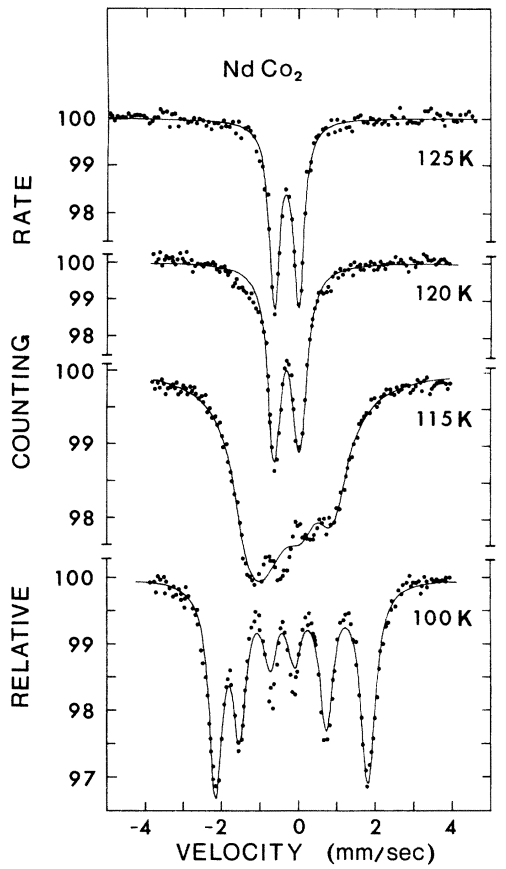

FIG. 3. Mössbauer spectra of $NdCo_2$-^{57}Fe between 100 and 125 K. The least-squares fits (full lines) are [100] procedure I simulations at 100, 115, and 120 K. At 125 K a vanishing effective hyperfine field was assumed. The blurred 115 K spectrum and the observed "wings" of the 120-K spectrum are discussed in the text.

Pattern *A* is a procedure I [110] fit, i.e., assuming two inequivalent sites with a 2 : 2 population ratio. Pattern *B* is also a two-site fit using procedure II, with *R*, the relative intensity of one site, as a free parameter. A procedure I [*uuw*]-type fit to the same spectrum is given by *C*. An inadequate fit was obtained using a procedure I [111] simulation. Corrections were made for a broadening of the absorption lines due to both the random iron occupation of the Co sites and ^{57}Fe saturation effects. These corrections prove to be negligible and of insignificant dependence on the iron content and did not improve the fit to the intensities of the innermost lines. Though *A*, *B*, and *C* of Fig. 1 are of similar quality, one notes that the [110] fit (*A*) fails to display some of the finer experimental details. Furthermore, fit *B* (Fig. 1) with $R = 0.56$ is physically unsound, since the presence of two inequivalent Co sites is due either to a [110] or to a [111] axis of $\vec{n}$, yielding a 2 : 2 or 3 : 1 population ratio ($R = 0.50$ or 0.75), respectively. However, the similarity between the fits of Fig. 1 suggests that $\vec{n}$, at 20 K, is close though not parallel to the [110] cubic axis. If $\vec{n}$ is contained in the $(1\bar{1}0)$ plane, as the [*uuw*] pattern (*C* in Fig. 1) implies, then two of the three [*uuw*] sites experience effective hyperfine fields of similar magnitude. Moreover, it is possible that $\vec{n}$ in $NdCo_2$ is not confined to a cubic symmetry plane so that four inequivalent Co sites are obtained. This possibility could not be verified using the present Mössbauer data. Evidently, a four-site fit, using more parameters, should be at least as adequate as the two- and three-site fits of Fig. 1.

The 43.5-K spectrum (Fig. 2) was fitted by a two-site procedure II simulation. The resulting $R = 0.65$, as compared with $R = 0.56$ of the corresponding 20-K fit (*B* in Fig. 1), illustrates the increasing deviation of $\vec{n}$ from the [110] axis, as the temperature approaches the ordered-state

transition region. This trend in the temperature dependence of $\vec{n}$ is further reflected in the procedure I [110] simulations of the $NdCo_2$-^{57}Fe Mössbauer spectra below 43.5 K. The quality of these fits improves with decreasing temperature, even though $\vec{n}$ does not align itself completely along the [110] axis above 4.2 K. The 44- and 44.5-K spectra (Fig. 2) could be fitted adequately by procedure I [*uuw*] simulations only. This implies an increasing deviation of $\vec{n}$ from the [110] axis close to the ordered-state transition temperature, so that the two-site appearance of the corresponding Mössbauer spectra is completely lost. Between 45 K (Fig. 2) and T_C (Fig. 3), $\vec{n}$ is along the [100] cubic axis. The occurrence of the blurred spectra just short of T_C (Fig. 3) is attributed to an increasingly dominating indirect Fe-Fe interaction—as the R-Co and Co-Co exchange is rapidly decreasing. Procedure I computer fits of the [100] type were applied to the spectra for $45 \leq T \leq 120$ K, and effective hyperfine fields with a reasonable temperature dependence, even close to T_C, were obtained (Fig. 4).

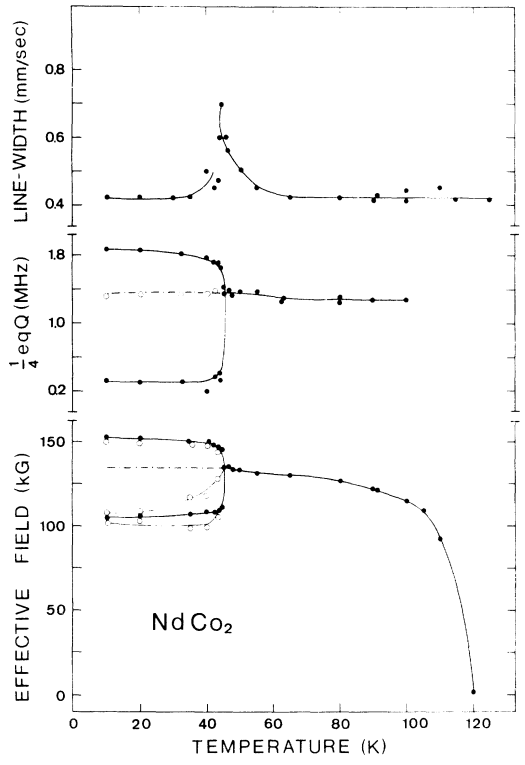

FIG. 4. Mössbauer line width, quadrupole interactions, and effective hyperfine fields of ^{57}Fe in $NdCo_2$ as a function of temperature. The presented values are obtained by least-squares computer simulations of the experimental Mössbauer spectra. Below 45 K both [*uuw*] procedure I fits (open circles) and two-site procedure II fits (full circles) were applied. The intensity-weighted averages of the quadrupole interactions and effective hyperfine fields, below 45 K, are shown by the dashed lines. Above 45 K [100] procedure I fits were applied.

TABLE II. Room-temperature quadrupole interaction and isomer shift of ^{57}Fe in $NdCo_2$ and $HoCo_2$.

	$NdCo_2$-^{57}Fe	$HoCo_2$-^{57}Fe
Quadrupole interaction (MHz)	3.59 ± 0.02	3.23 ± 0.02
Isomer shift (mm/sec)	−0.29 ± 0.02	−0.47 ± 0.02

The temperature dependence of the hyperfine constants of ^{57}Fe in $NdCo_2$, as obtained by the least-squares fits of the various applied types, is shown in Fig. 4. The intensity-weighted average of the two hyperfine effective fields H_{eff}, below 43.5 K, as obtained by procedure II fits, coincides with an extrapolation to low T of the H_{eff}-vs-T curve of the single iron site present above 45 K. It should further be noted in Fig. 4, that two of the three [*uuw*] hyperfine effective fields,

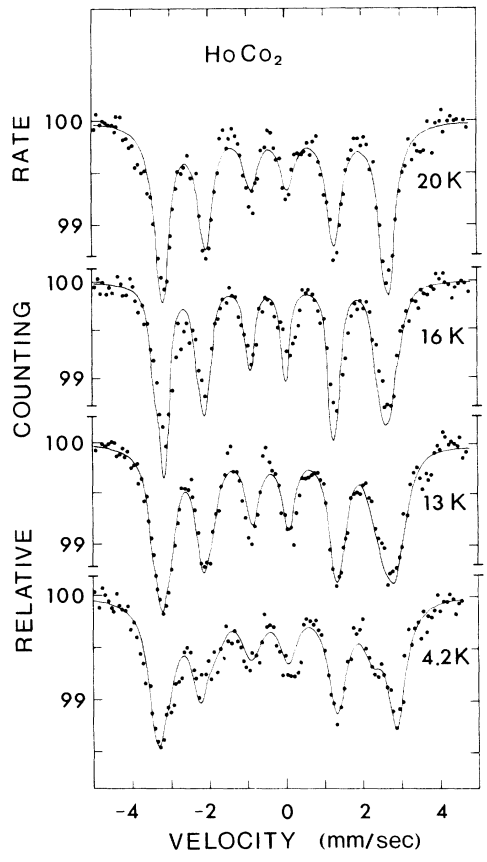

FIG. 5. Mössbauer spectra of $HoCo_2$-^{57}Fe between 4.2 and 20 K. The least-squares fits (full lines) are [111] procedure I type at 4.2 K; [*uuw*] procedure I type at 13 and 16 K; and [100] procedure I type at 20 K.

nearly coincide below 30 K. As the temperature approaches 45 K, the difference between the [*uuw*] fields becomes noticeable. The weighted average of the quadrupole interaction constants of the procedure II two-site fits below 43.5 K, coincides with both the single [*uuw*] $\frac{1}{4}eqQ$ below 43.5 K and the extrapolation to low T of the [100] $\frac{1}{4}eqQ$ vs T curve above 45 K (Fig. 4). The T dependence of the Mössbauer linewidth (Fig. 4) was obtained by [100] fits above 45 K and by procedure II fits below 45 K. The anomaly in the Γ_0 vs T curve at 45 K, illustrates the inadequacy of the two-site fits at temperatures close to 45 K. The similarity between the linewidths above 50 and below 40 K supports, however, the validity of the procedure II two-site fits below 40 K. The room-temperature isomer shift and quadrupole constant of ^{57}Fe in $NdCo_2$ are listed in Table II.

B. $HoCo_2$

The temperature dependence of the $HoCo_2$-^{57}Fe Mössbauer spectra reveals two magnetic transitions at[3] 16 K and at T_C. Mössbauer spectra corresponding to the ordered-state transition and to the order-disorder phase change are shown in Figs. 5 and 6, respectively. As in the case of $NdCo_2$ several trial computer fits were made. At 4.2 K, fits of both the [*uuw*] and [111] type were found to be adequate and of similar quality. Figure 5 displays the procedure I [111] fit at 4.2 K. As the temperature approaches 16 K, only fits of the [*uuw*] type were found to be satisfactory. Above 16 K simple six-line [100] patterns are obtained. The 20-K (Fig. 5) and the 75- and 90-K spectra (Fig. 6) represent this type of pattern and were fitted accordingly. At 95 K (Fig. 6), a quadrupole-split doublet was recorded.

Figure 7 presents the temperature dependence of the hyperfine effective fields in $HoCo_2$. Below 16 K, as $\vec{n}$ is evidently close though not parallel to the [111] cubic axis, both the [*uuw*] and the [111] hyperfine fields are shown. It is noticeable that the [111] fits yield H_{eff} with a reasonable T dependence below 10 K, whereas between 10 and 16 K, the [*uuw*] fits seem to produce better results. Above 16 K, $\vec{n}$ is parallel to the [100] cubic axis, and H_{eff}, as obtained by [100] fits, is shown. Noteworthy is the rapid decrease of H_{eff} of $HoCo_2$

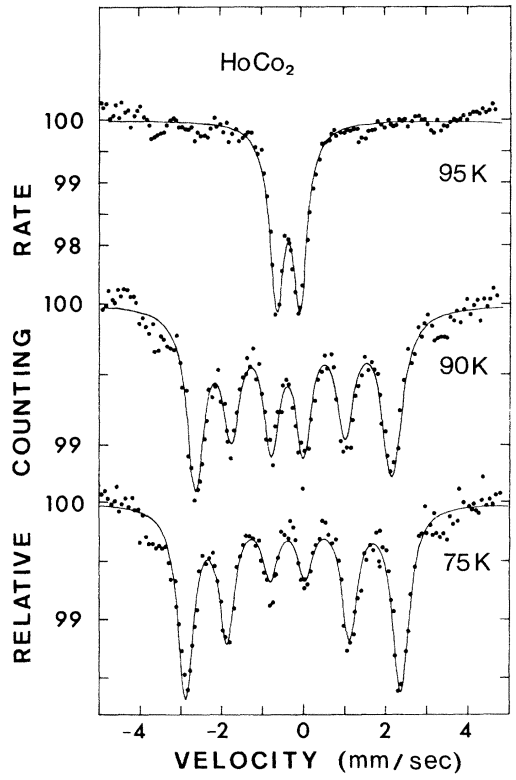

FIG. 6. Mössbauer spectra of $HoCo_2$-^{57}Fe between 75 and 95 K. The least-squares fits (full lines) are [100] procedure I simulations at 75 and 90 K. At 95 K a vanishing effective hyperfine field was assumed.

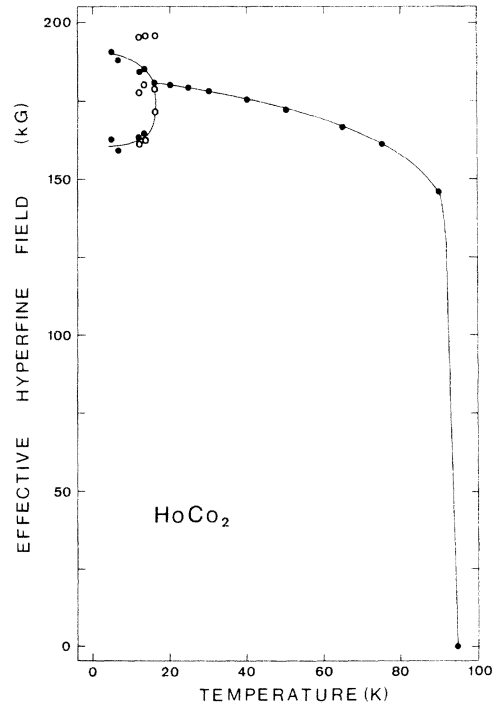

FIG. 7. Hyperfine effective fields of ^{57}Fe in $HoCo_2$ as a function of temperature. The presented values are obtained by least-squares computer simulations of the experimental Mössbauer spectra. Below 16 K both [*uuw*] procedure I fits (open circles) and [111] procedure I fits (full circles) were applied. Above 16 K, [100] procedure I fits were applied.

between 90 and 95 K (Fig. 7), as compared with the smooth temperature dependence of H_{eff} of $NdCo_2$, close to T_C (Fig. 4). The magnetic moments of the two compounds have been found to possess a similar temperature dependence, which was interpreted as corresponding to a first-order transition in $HoCo_2$,[25] and a random order-disorder transition in $NdCo_2$. The lattice and induced quadrupole constants obtained for $HoCo_2$ at 4.2 K are 1.30 ± 0.02 and 0.65 ± 0.02 MHz, respectively. Similar quadrupole constants are obtained at higher temperatures up to T_C. The room-temperature isomer shift and quadrupole constant of ^{57}Fe in $HoCo_2$ are listed in Table II. In both $NdCo_2$ and $HoCo_2$, the ^{57}Fe quadrupole constant above T_C (Table II) is much larger than the ordered-state value. The Mössbauer absorption linewidth in $HoCo_2$ is comparable with that of $NdCo_2$ (Fig. 4): $\Gamma_0(HoCo_2\text{-}^{57}Fe) = 0.54$ mm/sec at 4.2 K.

V. DISCUSSION

Some of the spin rotations in binary and ternary cubic Laves RFe_2 compounds[11-16] were described using the single-ion model.[15-17] Single-ion calculations which previously reproduced experimental spin-orientation diagrams[15] were recently expanded to yield also nonmajor symmetry axes of easy magnetization.[17] The observed spin rotations in $NdCo_2$ and $HoCo_2$ will be treated similarly. The Hamiltonian of a single rare-earth ion in a crystal is

$$\mathcal{H} = E_J I + \mathcal{H}_{\text{exc}} + \mathcal{H}_{\text{crys}}, \tag{1}$$

where E_J is the energy of the state J and I is the unit operator. The exchange Hamiltonian is

$$\mathcal{H}_{\text{exc}} = 2(g_J - 1)\mu_B H_{\text{exc}} \vec{J} \cdot \vec{n}.$$

It is assumed that the exchange interaction is isotropic and that the magnetocrystalline anisotropy of the rare-earth-containing alloy is due to the $4f$–crystal-field interaction. In order to treat a crystal-field-induced mixture of the first excited J state into the ground state of the R^{3+} ion, Racah operators U_i^j will be used for the crystal-field Hamiltonian. This is of importance in the case of light Nd^{3+}, and evidently negligible for heavy Ho^{3+}. These crystal-field effects have been verified by the magnetization measurements of $NdCo_2$,[6,7] and $HoCo_2$.[6,8-10] Thus

$$\mathcal{H}_{\text{crys}} = V_4 + V_6,$$

and

$$V_4 = A_4(1 - \sigma_4)\langle r^4\rangle[U_4^0 + \sqrt{\tfrac{5}{14}}(U_4^4 + U_4^{-4})],$$

$$V_6 = A_6\langle r^6\rangle[U_6^0 + \sqrt{\tfrac{7}{2}}(U_6^4 + U_6^{-4})].$$

A_4 and A_6 are crystal-field parameters. Previously calculated $\langle r^n\rangle$,[20] and shielding parameters σ_4,[21] were used. The Hamiltonian (1) was calculated and diagonalized for $\vec{n}$ parallel to the three major axes of cubic symmetry, as well as for various directions of $\vec{n}$ in the $(1\bar{1}0)$ and (001) planes. The free energy per ion is

$$F(\vec{n}, T) = -kT \ln Z(\vec{n}, T) = -kT \ln\left(\sum_{i=1}^{m} e^{-E_i/kT}\right), \tag{2}$$

where E_i are the eigenvalues of the single-ion Hamiltonian and $m = \sum_J (2J+1)$ is the number of energy levels. The easy axis of magnetization for a given R^{3+} ion at a given temperature is that for which the free energy (2) is a minimum.

Previous studies[15-17] have shown that the direction of $\vec{n}$ and its temperature dependence are very sensitive to the values of A_4 and A_6/A_4 and weakly dependent on the value of H_{exc}. In the present calculation, sets of A_4 and A_6/A_4 were obtained, which reproduce the experimental spin-rotation data for $NdCo_2$ and $HoCo_2$. The exchange field, experienced by the R^{3+} ion in RCo_2, can be estimated using the molecular-field approximation for the Curie temperature.[22] Since the dominant exchange interaction in the RCo_2 alloy is between the R and Co sublattices, and assuming a high-spin Co^{3+} with quenched orbital moment, we find $|H_{\text{exc}}| \approx 100$ K. This estimated H_{exc} is smaller than the 130-K,[16] or 150-K,[15] values estimated for RFe_2 alloys, in which the Fe-Fe exchange is dominating, and larger than $|H_{\text{exc}}| = 70$ K in RAl_2,[23] where R-R is the dominant exchange. The present calculations were repeated for several H_{exc} between 70 and 150 K. As expected, an insignificant dependence of the calculated easy axis of $\vec{n}$ on H_{exc}, in this range, was observed. The presented results were obtained with $|H_{\text{exc}}| = 100$ K for both $NdCo_2$ and $HoCo_2$. From the temperature depen-

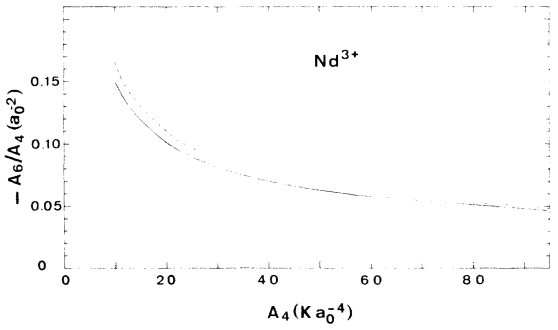

FIG. 8. Nd^{3+} single-ion calculated $-A_6/A_4$ vs A_4, which yield a [110] to [100] spin rotation at 43 ± 2 K in $NdCo_2$ (solid line). The dashed line presents crystal fields which produce a similar rotation at 50 ± 2 K. $|H_{\text{exc}}| = 100$ K was assumed.

dence of the magnetization and of the Mössbauer hyperfine fields in $HoCo_2$ and $NdCo_2$ (Figs. 4 and 7), this value is virtually temperature independent at least up to 20 K below T_C of each compound.

The solid line in Fig. 8 represents the crystal-field parameters for which a [110] to [100] spin rotation occurs at 43 ±2 K in $NdCo_2$, using $|H_{exc}| = 100$ K. The dashed line (Fig. 8) represents crystal-field parameters for which a similar rotation is obtained at 50 K. It demonstrates the sensitivity of the calculated results to the crystal-field parameters employed. To within 2 K off the spin-rotation temperature, only major symmetry axes of $\vec{n}$ were obtained. This is in agreement with the experimental results, which indicate a very narrow spin-rotation temperature interval in $NdCo_2$, around 43 K. In contrast to the Mössbauer data, which reveal a slight deviation of $\vec{n}$ from the [110] cubic axis below 43 K, the present calculations establish $\vec{n} \parallel [110]$ for $T < 41$ K. This inconsistency could not be removed by changing A_4 and A_6/A_4 over a large interval. For the Ho^{3+} ion completely different crystal-field parameters had to be used to reproduce the experimental $HoCo_2$ spin-orientation results. While negative A_6 were used for $NdCo_2$ (Fig. 8), a [111] easy axis of magnetization in $HoCo_2$ can be accounted for by positive A_6 only and relatively large A_6/A_4. A [111] to [100] spin rotation in $HoCo_2$ is obtained with $10 < A_4 < 45$ Ka_0^{-4} (a_0 is the Bohr radius) and $0.24a_0^{-2} < A_6/A_4 < 0.25a_0^{-2}$. The spin-rotation temperature is very sensitive to the crystal-field parameters employed. For $A_4 = 36$ Ka_0^{-4}, the $HoCo_2$ [111] to [100] spin rotation at 16 K is reproduced with $A_6/A_4 = 0.240455a_0^{-2}$. The calculated spin-rotation temperature interval is always very narrow (~1 K), in agreement with the experimental findings. As in the case of $NdCo_2$, nonmajor symmetry directions of $\vec{n}$ could not be obtained for Ho^{3+} over a 4.2–300-K interval. They present single-ion calculations assuming $|H_{exc}| = 100$ K.

The R-Co interaction is evidently not the only source of magnetocrystalline anisotropy, and additional contributions to the anisotropy free energy are present. These might cause the observed slight deviation of $\vec{n}$ from the [110] axis in $NdCo_2$ below 43 K, and the deviation of $\vec{n}$ from the [111] axis in $HoCo_2$ below 16 K. These deviations, from major axes of cubic symmetry, have been shown to be consistent with the cubic symmetry.[14,17] Apart from being negative in $NdCo_2$ and positive in $HoCo_2$, $|A_6/A_4|$ is larger for both the Nd and Ho compounds than for most of the RFe_2 alloys.[15,17] In previous calculations[15,17] $A_4 = 36$ Ka_0^{-4} and $A_6 = -0.038a_0^{-2}$ were successfully used for all the heavy-rare-earth ions in binary and ternary RFe_2 alloys. Though significantly larger crystal fields were applied in spin-rotation[16] and magnetization[24] studies of $SmFe_2$, positive A_4 and negative A_6 were obtained. We do not have an explanation for the occurrence of so extremely different crystal fields in isoelectronic and isostructural $NdCo_2$ and $HoCo_2$. Since the R-Co is the dominating exchange in RCo_2 alloys, it is possible that the crystal fields are very sensitive to the type of rare-earth ion, more than in the corresponding RFe_2 compounds. Further Mössbauer and magnetization studies of the RCo_2 compounds are currently underway.

ACKNOWLEDGMENTS

Thanks are due to D. Cohen, M. Ziv, J. Mazor, and S. Natan for their able technical assistance.

*Also at Materials Engineering Department, Ben-Gurion University, Beer-Sheva, Israel.

†Present address: Lawrence Berkeley Laboratory, University of California, Berkeley Calif. 94720.

[1]K. N. R. Taylor, Adv. Phys. 20, 551 (1971).

[2]C. Deenadas, R. S. Craig, N. Marzouk, and W. E. Wallace, J. Solid State Chem. 4, 1 (1972).

[3]J. Voiron, A. Berton and J. Chaussy, Phys. Lett. A 50, 17 (1974).

[4]J. Farrell and W. E. Wallace, Inorg. Chem. 5, 105 (1966).

[5]R. Lemaire, Cobalt 33, 201 (1966).

[6]E. Burzo, Int. J. Magn. 3, 161 (1973).

[7]J. M. Machado da Silva, J. M. McDermott, and R. W. Hill, J. Phys. C 5, 1573 (1972).

[8]D. Bloch, J. Voiron, A. Berton, and J. Chaussy, Solid State Commun. 12, 685 (1973).

[9]R. M. Moon, W. C. Koehler, and J. Farrell, J. Appl. Phys. 36, 978 (1965).

[10]J. Voiron, C. R. Acad. Sci. (Paris) 274, 589 (1972).

[11]G. Dublon, U. Atzmony, M. P. Dariel, and H. Shaked, Phys. Rev. B 12, 4628 (1975).

[12]U. Atzmony, M. P. Dariel, E. R. Bauminger, D. Lebenbaum, I. Nowik, and S. Ofer, *Proceedings of the Tenth Rare-Earth Conference, Carefree, Arizona, 1973,* edited by C. J. Kevane and T. Moeller (U.S. AEC, Oak Ridge, Tenn., 1973), p. 605.

[13]U. Atzmony and M. P. Dariel, Phys. Rev. B 10, 2060 (1974).

[14]U. Atzmony and M. P. Dariel, AIP Conf. Proc. 24, 662 (1974).

[15]U. Atzmony, M. P. Dariel, E. R. Bauminger, D. Lebenbaum, I. Nowik, and S. Ofer, Phys. Rev. B 7, 4220 (1973).

[16]A. M. van Diepen, H. W. de Wijn, and K. H. J. Buschow, Phys. Rev. B 8, 1125 (1973).

[17]U. Atzmony and M. P. Dariel, Phys. Rev. B 13, 4006 (1976).

[18]M. Rosen (private communication).
[19]H. Pinto and H. Shaked (private communication).
[20]A. J. Freeman and R. E. Watson, Phys. Rev. 127, 2058 (1962).
[21]A. J. Freeman and R. E. Watson, Phys. Rev. 139, A1606 (1965).
[22]L. Neél, Ann. Phys. (Paris) 3, 137 (1948).
[23]H. W. de Wijn, A. M. van Diepen, and K. H. J. Buschow, Phys. Rev. B 7, 524 (1973).
[24]G. Dublon, M. P. Dariel, and U. Atzmony, Phys. Lett. A 51, 262 (1975).
[25]D. Bloch, D. M. Edwards, M. Shimizu, and J. Voiron, J. Phys. F 5, 1217 (1975).